ARTICLE

Comparative Analysis of Hydration Layer Reorientation Dynamics of Antifreeze Protein and Protein Cytochrome P450†

Hongfeng Yu[a,b], Qiang Zhang[c*], Wei Zhuang[a,d*]

a. State Key Laboratory of Structural Chemistry, Fujian Institute of Research on the Structure of Matter, Chinese Academy of Sciences, Fuzhou 350002, China
b. University of Chinese Academy of Sciences, Beijing 100049, China
c. College of Chemistry and Material Sciences, Inner Mongolia Minzu University, Tongliao 028043, China
d. Institute of Urban Environment, Chinese Academy of Sciences, Xiamen 361021, China

(Dated: Received on March 10, 2022; Accepted on April 28, 2022)

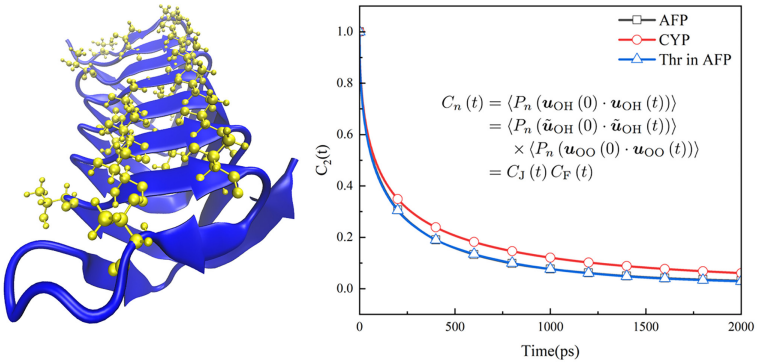

Antifreeze proteins (AFPs) inhibit ice recrystallization by a mechanism remaining largely elusive. Dynamics of AFPs' hydration water and its involvement in the antifreeze activity have not been identified conclusively. We herein, by simulation and theory, examined the water reorientation dynamics in the first hydration layer of an AFP from the spruce budworm, *Choristoneura fumiferana*, compared with a protein cytochrome P450 (CYP). The increase of potential acceptor water molecules around donor water molecules leads to the acceleration of hydrogen bond exchange between water molecules. Therefore, the jump reorientation of water molecules around the AFP active region is accelerated. Due to the mutual coupling and excitation of hydrogen bond exchange, with the acceleration of hydrogen bond exchange, the rearrangement of the hydrogen bond network and the frame reorientation of water are accelerated. Therefore, the water reorientation dynamics of AFP is faster than that of CYP. The results of this study provide a new physical image of antifreeze protein and a new understanding of the antifreeze mechanism of antifreeze proteins.

Key words: Hydration layer, Antifreeze protein, Reorientation dynamics

I. INTRODUCTION

The structure and dynamics of the protein hydration layer play an important role in the realization of protein biological function [1–6], such as protein folding, ligand binding, and protein recognition. Antifreeze proteins (AFP) are a special family of proteins with the ability to reduce the growth temperature of ice crystals [7]. It widely exists in some plants [8], fish [9], fungi [10] and bacteria [11] living in the sub-zero temperature areas on earth. Understanding the antifreeze mechanism of AFP has broad application potentials, such as improving the cold tolerance of plants through genetic engineering [12]

†Part of Special Topic "Quantum and Classical Dynamics in Chemistry" in the 32nd Chinese Chemical Society Congress.
*Authors to whom correspondence should be addressed. E-mail: qzhang@imun.edu.cn, wzhuang@fjirsm.ac.cn

 ©2022 Chinese Physical Society

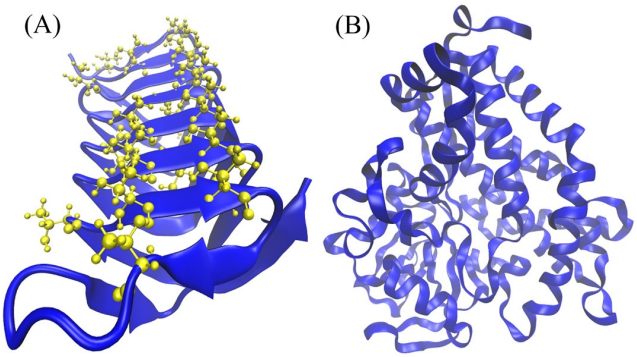

FIG. 1 Chemical structures of (A) AFP, with the two rows of Thr residues (yellow) on the ice-binding face represented explicitly, and (B) cytochrome P450 (CYP).

and the low-temperature preservation technology of human organs [13]. As an important aspect of this mechanism, the hydration dynamics of AFPs and their role in antifreeze activity, however, remain largely elusive.

Here, we examined the water dynamics in the first hydration layer of an AFP from the spruce budworm *Choristoneura fumiferana* and a protein cytochrome P450 (CYP), by simulations. The ice-binding surface of AFP has been identified by NMR and mutations experiments and was characterized by its very flat topography, with threonine residues forming two parallel rows on the surface [14]. The chemical structures of these materials are presented in FIG. 1. The mutation studies showed that replacing threonine residues in the active region by leucine reduces the antifreeze activity by 80%−90% [15], while replacing threonine in the inactive region has little or no effect, which indicates the important role of threonine residues in the active region. We, therefore, studied the water dynamics within the first hydration layer of these threonine residues as a further comparison.

We mainly studied the reorientation time of hydrated water through the second-order Legendre polynomial time correlation function. The results showed that the reorientation time of water in the first hydration layer of the AFP active region is faster than that of CYP. To explain the result, we decomposed the reorientation of water into a jump reorientation and a frame reorientation with the help of the extended jump model [16–19]. A higher density of potential acceptor around the hydrogen bond donor is observed for the water on the surface of AFP, so it is easier for the hydrogen bond donor to switch its acceptor than CYP. A more compact and extensive hydrogen bond network around hydration sites of AFP results in a higher possibility for water hydrogen to switch its hydrogen bond between water molecules hydrogen-bonded each other with a smaller jump angle than around CYP. On the other hand, the hydrogen bond exchange reaction is highly coupled among the percolated hydrogen bonds in the hydrogen bond network [20], so an activated hydrogen bond can accelerate its neighbors, and then make the relaxations of the hydrogen bond network and hydration dynamics fast. As a result, the frame reorientation of the hydrogen bond pair near AFP is enhanced compared to CYP. In all, the jump reorientation and frame reorientation of AFP are faster than that of CYP, which eventually leads to an acceleration of water reorientation.

II. METHODOLOGY

A. Simulation details

The initial structure of the spruce budworm Choristoneura fumiferana antifreeze protein for simulations was taken from the PDB crystal structure (1z2f) [14]. Three protein monomers were filled in a cubic box. 836 water molecules were inserted into the box randomly to reach a mass ratio of 0.4 g water/1 g protein, which mimics the experimental condition. Then 6 chlorine counter ions were added into the simulation box to keep the system neutral in charge. The CHARMM 27 force field in the GROMACS package was used for AFP. The TIP4P/Ew model was chosen for water [21]. After the 5000 steps energy minimization procedure, a 10 ns NVT equilibration simulation was carried out at each temperature. The product simulations were then carried out for 30 ns with constant volume and composition. An initial velocity of each atom was set based on a Maxwell distribution at the desired temperature. All bonds of water in the simulation were constrained with the LINCS algorithm to maintain their equilibration length [22]. The system was propagated using the leap-frog integration algorithm [23] with a time step of 2 fs. The electrostatic interactions were calculated using the Particle Mesh Ewald (PME) [24] method. A non-bond pair-list cutoff of 1 nm was used and the pair-list was updated every 20 fs. The initial structure of protein cytochrome P450 (CYP) for simulations was taken from the PDB crystal structure (1dz9) [25]. Two protein monomers were filled in a cubic box. 2025 water molecules were inserted into the box randomly to reach a mass ratio of 0.4 gram water/1 gram protein. Then 34 sodium counter ions were added into the simu-

DOI:10.1063/1674-0068/cjcp2203038 ©2022 Chinese Physical Society

lation box to keep the system neutral in charge. Other conditions were the same as AFP.

B. Analysis of water dynamics

1. Orientational correlation functions

By analyzing the molecular dynamics trajectory, we obtained the position analytical analysis of water reorientation dynamics in protein hydrated shells. The reorientation of each water molecule was monitored by following the dynamics of the water OH-bond vector $\boldsymbol{u}$, through the second-order Legendre polynomial time-correlation function (tcf) [26, 27]

$$\begin{aligned} C_n(t) &= \langle P_n(\boldsymbol{u}_{\mathrm{OH}}(0)\cdot\boldsymbol{u}_{\mathrm{OH}}(t))\rangle \\ &= \langle P_n(\tilde{\boldsymbol{u}}_{\mathrm{OH}}(0)\cdot\tilde{\boldsymbol{u}}_{\mathrm{OH}}(t))\rangle \\ &\quad\times\langle P_n(\boldsymbol{u}_{\mathrm{OO}}(0)\cdot\boldsymbol{u}_{\mathrm{OO}}(t))\rangle \\ &= C_{\mathrm{J}}(t)\,C_{\mathrm{F}}(t) \end{aligned} \tag{1}$$

$\tilde{\boldsymbol{u}}_{\mathrm{OH}}$ is the unit vector of water OH bond within the local OA frame of hydrogen bond and $\boldsymbol{u}_{\mathrm{OO}}$ is the orientation of hydrogen bond frame OA (A represents the heavy atom in the hydrogen bond receptor, which can be the oxygen atom of water, the nitrogen atom and the oxygen atom of protein.). $C_{\mathrm{J}}(t)$ and $C_{\mathrm{F}}(t)$ are the jump and frame orientation correlation functions.

The results can correspond to the anisotropic attenuation of ultrafast infrared spectroscopy and the directional relaxation time of magnetic relaxation technology [26]. In the bulk, the relaxation of $C_2(t)$ is exponential at room temperature, but it shows obvious non-single exponential attenuation at a supercooling temperature [28].

2. The hydrogen bond correlation function

The hydrogen bond switching event begins with the stable hydrogen bond state of $\mathrm{O}^*{-}\mathrm{H}^*\cdots\mathrm{O}^{\mathrm{a}}$ and ends with the stable product state $\mathrm{O}^*{-}\mathrm{H}^*\cdots\mathrm{O}^{\mathrm{b}}$. The hydrogen bond correlation function is [16, 18, 19]

$$C_{\mathrm{H}}(t) = 1 - \left\langle n_i^{\mathrm{R}}(0)\, n_j^{\mathrm{R}}(t)\right\rangle \tag{2}$$

The hydrogen bond state functions, $n_i^{\mathrm{R}}(0)$ and $n_j^{\mathrm{R}}(t)$ are equal to 0 at the stable reactant state and equal to 1 at the stable product state. $C_{\mathrm{H}}(t)$ represents the probability of forming a stable product at time t when the system is in the reactant state at t=0. The conditions for the formation of hydrogen bonds between two molecules are considered to be $R_{\mathrm{O^*A}}$<3.1 Å, $R_{\mathrm{H^*A}}$<2.0 Å and the hydrogen bond angle $\theta_{\mathrm{H^*O^*A}}$<20° [16, 17]. H^* and O^* are the hydrogen and oxygen atoms from the hydrogen-bond donor water.

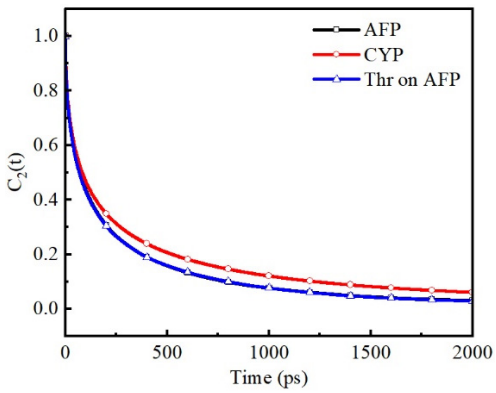

FIG. 2 Water (second-order Legendre polynomial) orientational time correlation function: AFP (black), CYP (red), and Thr residues on AFP (blue) at 245 K.

3. Asphericity

Among the different parameters characterizing the local tetrahedral order in water, the asphericity of Voronoi cells has a good correlation with jump time [28]. The library Voro++, by Rycroft *et al.* [29], serves as the basis for this analysis because the algorithms use independent construction of the Voronoi cells. The asphericity η of the cell is defined as [28, 30]

$$\eta = \frac{A^3}{36\pi V^2} \tag{3}$$

where V and A are the polyhedron volume and area. This parameter η increases from 1 for a spherical cell corresponding to a disordered shell with many nearest neighbors to 2.25 for a perfect ice-like arrangement.

III. RESULTS AND DISCUSSION

The reorientation dynamics of water in the first hydration layer of protein as an indicator is sensitive to the intrinsic properties of the protein interface. A series of molecular dynamic simulations were carried out to generate the trajectories of solvated AFP and CYP at 245 K (freezing point for the TIP4P/Ew water model used herein). Time-dependent reorientation correlation functions of water molecules initially in the first layer of the AFP protein, the CYP protein and the Thr residues of AFP as the active area on AFP, are extracted and shown in FIG. 2. All display a rapid initial libration

DOI:10.1063/1674-0068/cjcp2203038 ©2022 Chinese Physical Society

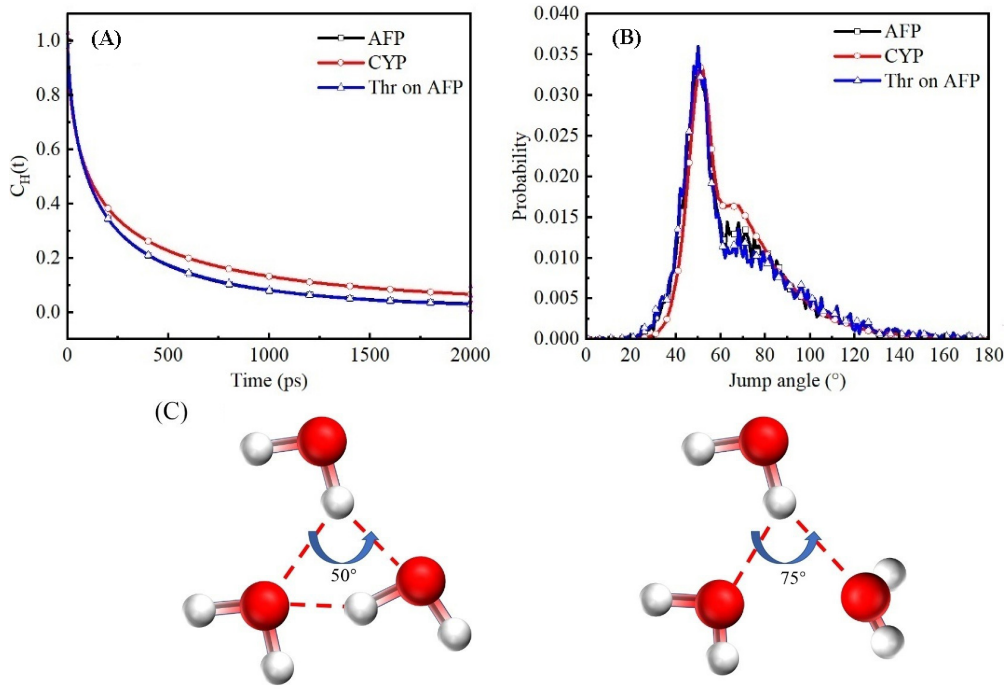

FIG. 3 (A) Hydrogen bond correlation function $C_{\mathrm{H}}(t)$ of water-water hydrogen bond for water around AFP (black), CYP (red) and Thr residues on AFP (blue) at 245 K. (B) Jump angle distribution, determined as a cut in the distribution of $\Phi_{\mathrm{O^aO^*O^b}}$ values when the jump occurs. (C) The geometries of the hydrogen bond transition state correspond to the 50° and 75° characteristic jump angle.

decay, followed by a slower exponential decay. We note at this stage that the reorientation time of water on AFP's first hydration shell is similar to that for the Thr residues case, but faster than the CYP case. The reorientation of water around AFP, especially around the active site of antifreeze AFP, is slower than that around CYP without antifreeze ability after a fast libration.

We next applied an extended molecular jump (EMJ) model to reveal the molecular mechanism of the different water reorientation behaviors observed. The details of this model were elaborated in a number of previously reported works [16–19]. In short, in the hydrogen bond network, the reorientation of water is mainly composed of a large-amplitude angular jump when hydrogen bond exchange occurs and a slow diffusive frame reorientation in the time interval between jumps. The total reorientation time of water can be written as a summation of two contributions:

$$\frac{1}{\tau_2} = \frac{1}{\tau_2^{\mathrm{jump}}} + \frac{1}{\tau_2^{\mathrm{frame}}}$$

According to the Ivanov model [31], the jump component of reorientation time of water, τ_2^{jump}, is calculated as:

$$\tau_2^{\mathrm{jump}} = \tau_0 \left[1 - \frac{1}{5} \frac{\sin\left(\frac{5\Delta\theta}{2}\right)}{\sin\left(\frac{\Delta\theta}{2}\right)} \right]^{-1} \tag{4}$$

where τ_0 is the hydrogen bond lifetime and $\Delta\theta$ is the angular jump amplitude. The jump reorientation of water is determined by the jump angle and hydrogen bond lifetime. In FIG. 3(A), we show hydrogen bond correlation function $C_{\mathrm{H}}(t)$ of water-water hydrogen bond for AFP, CYP and Thr residues on AFP at 245 K. The hydrogen bond lifetime of water molecules around the active region of AFP is shorter than that of CYP. We fitted the hydrogen bond correlation function with a single exponential function in the range of 1−2000 ps. The results give the hydrogen bond lifetime as $\tau_{0\text{-CYP}}$=302.11 ps, $\tau_{0\text{-AFP}}$=227.27 ps and $\tau_{0\text{-Thr}}$=228.31 ps. Water jump angle probability distributions of AFP, CYP, and Thr residues on AFP at 245 K are shown in FIG. 3(B). The jump angle is defined as the value of angle $\theta_{\mathrm{AO^*B}}$ at the moment of hydrogen bond jump. The jump angle distributions are asymmetric with a sharp peak centered at ∼50° and a broad shoulder at ∼75° with a long dif-

DOI:10.1063/1674-0068/cjcp2203038 ©2022 Chinese Physical Society

fusive tail. Compared with CYP, the sharp peak of AFP at ∼50° shifts slightly towards the smaller jump angle while the shoulder at ∼75° becomes less prominent. Two feature jump angles correspond to two different geometries at the transition state of hydrogen bond switching in FIG. 3(C), which also suggests a specific difference of hydrogen bond network structure of solvated water around AFP and CYP. The average values of jump angle of AFP, CYP and Thr residues on AFP are 64.56°, 65.84°, and 64.02°. Consequently, the jump reorientation times of CYP and AFP, τ_2^{jump}, are 334.84 ps and 258.07 ps respectively as Eq.(4), which indicate that the active region of AFP can effectively improve the rate of hydrogen bond switch of water molecules in hydration layer and enhance the reorientation of water. The results show that the hydrogen bond lifetime τ_0 plays a decisive role in the jump reorientation time compared to the jump angle according to the equation above. A longer hydrogen bond lifetime results in a longer jump reorientation time of water.

Hydrogen bond lifetime is affected not only by the strength of the hydrogen bond, but also by the accessibility of potential acceptors [32, 33]. In this research, the water-water hydrogen bonds at the same temperature have the same interaction energy for the two systems. We calculated the density distribution of potential acceptor water molecules around the donor water molecules before hydrogen bond exchange, as shown in FIG. 4. The results showed that the density of potential receptor water molecules around Thr residue in AFP is the highest, the active region of AFP is the second, and CYP is the lowest. The active layer of AFP can increase the surrounding potential receptor water molecules.

In addition, we also analyzed the local structural order of water molecules around the active region of AFP and CYP. The structure of the solvation shell surrounding each water molecule is probed by the asphericity of the Voronoi cell associated with water molecule [28]. This parameter increases from 1 for a spherical cell corresponding to a disordered shell with many nearest neighbors to 2.25 for a perfect ice-like arrangement. In FIG. 5, the asphericity of water molecules around AFP and Thr residues on AFP is closer to that of ice. The comparison of CYP and AFP shows that the hydration sites next to AFP are significantly more aspherical and more structured than those next to CYP. Therefore, the local hydrogen bond network structure of water molecules around the AFP active region is more orderly,

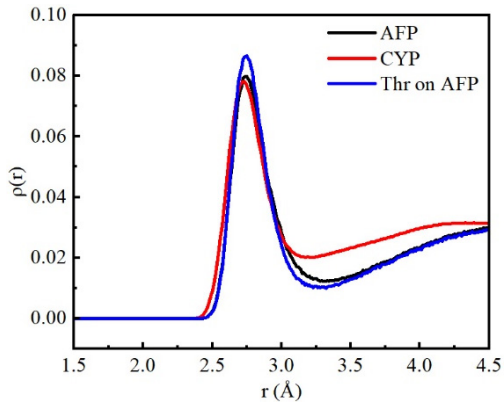

FIG. 4 The density distribution $\rho(r)$ of potential acceptor water molecules around the donor water molecules before hydrogen bond exchange around AFP (black), CYP (red), and Thr residues on AFP (blue) at 245 K.

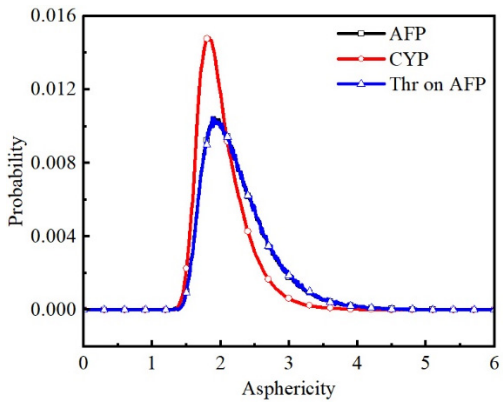

FIG. 5 Voronoi asphericity distributions of water molecules: AFP (black), CYP (red), and Thr residues on AFP (blue) at 245 K.

resulting in the hydrogen bond jump angle between water molecules tending to 50°. The increasing order of hydrogen bond network structure suggests that, in the process of hydrogen bond exchange, the old and new receptor water molecules are connected in the form of the hydrogen bond. We further calculated the probability of hydrogen bond formation, that is, at the moment of hydrogen bond jump, the hydrogen bond exchange event of hydrogen bond formation between new and old acceptor water molecules divided by all hydrogen bond exchange events. The results show that the hydrogen bonding probability of the first hydration layer around the Thr residue on AFP is the highest, which is 42.01%, followed by that of AFP, which is 40.54%, and that of CYP is the lowest, which is 33.73%. This indicates that the active region of AFP enhances the hydrogen bond network structure in its first hydration layer, making

DOI:10.1063/1674-0068/cjcp2203038 ©2022 Chinese Physical Society

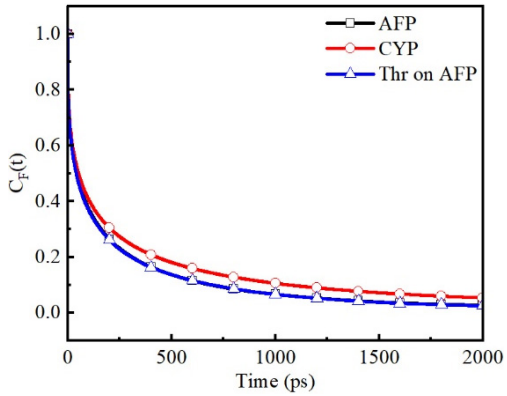

FIG. 6 Frame orientational time correlation function: AFP (black), CYP (red), and Thr residues on AFP (blue) at 245 K.

it less prone to large angle jumps, thus accelerating the jump reorientation time of water molecules. A percolating hydrogen bond network can accelerate the hydrogen bond exchange and the jump reorientation time of water.

Another contribution to the reorientation time of water is the frame reorientation time. The frame correlation function refers to the reorientation of the hydrogen bond frame O*A during the time interval between hydrogen bond jumps. FIG. 6 shows the frame orientational time correlation function, which indicates that the frame orientational time τ_n^{frame} of AFP, 192.30 ps, is faster than that of CYP, 258.40 ps. Unlike the fast jump component, which is decided by the nearest neighbors of the target water molecule, the frame reorientation as a slow diffusive component correlates with the collective structure rearrangement. However, the collective structure relaxation of liquid is also driven by molecule pair relaxation or basic solvation shell exchanges according to the mode-coupling theory [34]. In the current systems, the speed of hydrogen bond exchange remains a dominant and elementary process and determines the rate of the whole structural rearrangement. Besides this, hydrogen bond exchange is coupled with each other, while the hydrogen bond exchange accelerates, the hydrogen bond exchange network in the whole environment will also accelerate, resulting in the frame reorientation of the hydrogen bond pair [20].

IV. CONCLUSION

We herein studied water reorientation dynamics at the surface of an antifreeze protein and a non-antifreeze protein using the combination of molecular dynamics simulations and the extended molecular jump model. The increase of potential acceptor water molecules around donor water molecules around AFP, especially near Thr residues of AFP, leads to the acceleration of exchange between the water-water hydrogen bonds. Therefore, the jump reorientation of water molecules adjacent to the AFP active region is accelerated. Due to the mutual coupling, mutual excitation and mutual activation of the elementary process of hydrogen bond exchange, the rearrangement of the hydrogen bond network accelerates with the acceleration of hydrogen bond exchange, and the frame reorientation of water also accelerates. Therefore, the water reorientation dynamics of AFP is faster than that of CYP. The results of this study provide a new physical image of antifreeze protein and a new understanding of the antifreeze mechanism of the antifreeze protein.

V. ACKNOWLEDGMENTS

This work was supported by the National Natural Science Foundation of China (No.21873101 and No.22063007). Qiang Zhang thanks the support of the Natural Science Foundation of Inner Mongolia (No.2020MS02018) and Scientific Research Foundation of IMUN for doctors (BS581).

[1] B. Bagchi, Chem. Rev. **105**, 3197 (2005).
[2] P. Ball, Chem. Rev. **108**, 74 (2008).
[3] B. Halle, Philos. Trans. R. Soc. Lond. B Biol. Sci. **359**, 1207 (2004).
[4] Y. Levy and J. N. Onuchic, Annu. Rev. Biophys. Biomol. Struct. **35**, 389 (2006).
[5] S. K. Pal and A. H. Zewail, Chem. Rev. **104**, 2099 (2004).
[6] A. C. Fogarty, E. Duboue-Dijon, F. Sterpone, J. T. Hynes, and D. Laage, Chem. Soc. Rev. **42**, 5672 (2013).
[7] A. J. Middleton, C. B. Marshall, F. Faucher, M. Bar-Dolev, I. Braslavsky, R. L. Campbell, V. K. Walker, and P. L. Davies, J. Mol. Biol. **416**, 713 (2012).
[8] D. Worrall, L. Elias, D. Ashford, M. Smallwood, C. Sidebottom, P. Lillford, J. Telford, C. Holt, and D. Bowles, Science **282**, 115 (1998).
[9] A. L. Devries, Science **172**, 1152 (1971).
[10] C. H. Robinson, New Phytol. **151**, 341 (2001).
[11] J. A. Gilbert, P. J. Hill, C. E. R. Dodd, and J. Laybourn-Parry, Microbiology **150**, 171 (2004).
[12] Y. Fan, B. Liu, H. Wang, S. Wang, and J. Wang, Plant Cell Rep. **21**, 296 (2002).
[13] B. Rubinsky, A. Arav, and A. L. Devries, Cryobiology **29**, 69 (1992).

DOI:10.1063/1674-0068/cjcp2203038 ©2022 Chinese Physical Society

[14] C. Li, X. Guo, Z. Jia, B. Xia, and C. Jin, J. Biomol. NMR **32**, 251 (2005).
[15] S. P. Graether, M. J. Kuiper, S. M. Gagné, V. K. Walker, Z. Jia, B. D. Sykes, and P. L. Davies, Nature **406**, 325 (2000).
[16] D. Laage and J. T. Hynes, Science **311**, 832 (2006).
[17] D. Laage and J. T. Hynes, J. Phys. Chem. B **112**, 14230 (2008).
[18] Q. Zhang, H. Chen, T. Wu, T. Jin, Z. Pan, J. Zheng, Y. Gao, and W. Zhuang, Chem. Sci. **8**, 1429 (2017).
[19] Q. Zhang, T. Wu, C. Chen, S. Mukamel, and W. Zhuang, Proc. Natl. Acad. Sci. USA **114**, 10023 (2017).
[20] C. Liu, W. Li, and W. Wang, Phys. Rev. E **87**, 052309 (2013).
[21] H. W. Horn, W. C. Swope, J. W. Pitera, J. D. Madura, T. J. Dick, G. L. Hura, and T. Head-Gordon, J. Chem. Phys. **120**, 9665 (2004).
[22] B. Hess, H. Bekker, H. J. C. Berendsen, and J. G. E. M. Fraaije, J. Comput. Chem. **18**, 1463 (1997).
[23] S. Miyamoto and P. A. Kollman. J. Comput. Chem. **13**, 952 (1992).
[24] T. Darden, D. York, and L. Pedersen, J. Chem. Phys. **98**, 10089 (1993).
[25] I. Schlichting, J. Berendzen, K. Chu, A. M. Stock, S. A. Maves, D. E. Benson, R. M. Sweet, D. Ringe, G. A. Petsko, and S. G. Sligar, Science **287**, 1615 (2000).
[26] D. Laage, G. Stirnemann, F. Sterpone, R. Rey, and J. T. Hynes, Annu. Rev. Phys. Chem. **62**, 395 (2011).
[27] A. C. Fogarty and D. Laage. J. Phys. Chem. B **118**, 7715 (2014).
[28] G. Stirnemann and D. Laage. J. Chem. Phys. **137**, 031101 (2012).
[29] C. H. Rycroft, Chaos **19**, 041111 (2009).
[30] G. Ruocco, M. Sampoli, and R. Vallauri, J. Chem. Phys. **96**, 6167 (1992).
[31] E. N. Ivanov, J. Exp. Theor. Phys. **18**, 1041 (1964).
[32] D. Laage, G. Stirnemann, and J. T. Hynes. J. Phys. Chem. B **113**, 2428 (2009).
[33] X. Zhang, Z. Wang, Z. Chen, H. Li, L. Zhang, J. Ye, Q. Zhang, and W. Zhuang, J. Phys. Chem. B **124**, 1806 (2020).
[34] J. P. Hansen and I. R. McDonald, *Theory of Simple Liquids*, 2nd Edn., London: Academic Press, (1990).

DOI:10.1063/1674-0068/cjcp2203038 ©2022 Chinese Physical Society